



Generalized training subset selection for statistical estimation of epicardial activation maps from intravenous catheter measurements

Bülent Yılmaz*, Robert S. MacLeod

Biomedical Engineering Department, Başkent University, Ankara 06530, Turkey

Received 9 June 2005; accepted 15 March 2006

Abstract

Catheter-based electrophysiological studies of the epicardium are limited to regions near the coronary vessels or require transthoracic access. We have developed a statistical approach by which to estimate high-resolution maps of epicardial activation from very low-resolution multi-electrode venous catheter measurements. This technique uses a linear estimation model that derives a relationship between venous catheter measurements and unmeasured epicardial sites from a set of previously recorded, high-resolution epicardial activation-time maps used as a training data set based on the spatial covariance of the measurement sites. We performed 14 dog experiments with various interventions to create an epicardial activation-time map database. This database included a total of 592 epicardial activation maps which were recorded using a sock array placed on the ventricles of dog hearts. We present five approaches, which examined sequential addition and removal of maps to select a generalized training set for the estimation technique. The selection consisted of choosing a subset of epicardial ectopic activation-time maps from the database of beats which resulted in estimation accuracy levels better than or at least similar to using all the maps in database. Our aim was to minimize the redundancy in the database and to be able to guide the eventual procedures required to obtain training data from open-chest surgery patients. The results from this study illustrated this redundancy and suggested that by including an optimal subset (around 100 maps) of the full database the estimation technique was able to perform as well as and even in some cases better than including all the maps in the database. The results also suggest that such an approach is feasible for providing accurate reconstruction of complete epicardial activation-time maps in a clinical setting and with fewer maps we can obtain similar reconstruction accuracy levels.

© 2006 Elsevier Ltd. All rights reserved.

Keywords: Instance selection; Training set selection; Statistical estimation; Epicardial activation-time maps; Catheter mapping

1. Introduction

Heart rhythm disturbances, or “arrhythmias,” affect over four million Americans and are the cause of an estimated 500,000 deaths in the U.S. each year [1]. Therefore, the study and treatment of cardiac arrhythmias have major implications for public health.

Localization of the source of arrhythmias ranges from simple noninvasive body-surface electrograms (ECGs) to highly invasive open-chest epicardial and transmural electrical measurements. Cardiac mapping is the general term for collection of these methods. Cardiac mapping techniques that are limited to the endocardium are unsuccessful when arrhythmic

substrates are located deep in the subendocardium or in the subepicardium, which is the case in 15% of all ventricular arrhythmias [2]. Epicardial mapping using standard [3,4] specialized CARTO catheters [5] have been investigated and found to be highly efficient in this subgroup of patients. The disadvantage of both systems is that they require lengthy sequential mapping procedures and stable arrhythmias. In addition, the risk of hemopericardium has been reported in around 8% of the cases [6].

Another mapping approach targeting the epicardium uses the multielectrode catheters placed in the coronary veins [7,8]. These catheters (Cardima Inc., Fremont, CA, USA) have 4-to-20 electrodes on each and are small enough (outer diameter is around 0.8mm) to fit within the coronary veins. Their design permits insertion of multiple catheters using one guide-wire; therefore, simultaneous mapping of different regions of

* Corresponding author. Tel.: +90 312 234 1010x1464; fax: +90 312 234 1051.

E-mail address: byilmaz@baskent.edu.tr (B. Yılmaz).

the heart is possible. However, transvenous signals from multi-electrode catheters are limited to nearby regions in approximately 2 mm vicinity, missing most of the epicardium.

To overcome this limitation, we developed a statistical estimation technique to reconstruct the activation pattern over the entire epicardium using highly sparse venous catheter electrode recordings. The technique was a linear least-squares estimator based on a set of previously recorded, high-resolution epicardial activation-time maps used as a training data set. The spatial covariance computed from the training set derives a relationship between the venous catheter measurements and unmeasured epicardial sites; therefore the training set becomes a key component in this approach.

We previously showed that signal morphology and activation time values from venous catheters recordings were highly correlated with those from nearby epicardial sites [9]. We selected a subset of electrodes that lay near the coronary veins from a high-resolution epicardial electrode array and treated them as surrogates for true catheter measurements. Flexibility in surrogate electrode number and placement was thereby possible while still creating realistic conditions for potential clinical applications of the technique.

In the preliminary step of our research [10] with fewer maps in the database, we found that selection of the training data set had a bearing on the accuracy of the resulting estimation and set out to examine this behavior in more detail. We wished to address systematically the relationship between training data set selection and estimation accuracy. This topic has challenged investigators for many years in a large number of application areas, for example, pattern recognition [11–14], pattern classification [15,16], medical image segmentation [17], and remote sensing [18–20]. We followed two paths in the training data set selection problem; (1) “case-specific training data set selection” methods, which examined the optimal content of a training set for each map to be reconstructed individually, and (2) “generalized training data set selection” methods, which consisted of choosing a subset of epicardial activation maps from a database that could be used in all possible test cases. We reported the results from the first approach in Ref. [21]. In this particular study, we concentrated on the second approach in training data set selection for statistical estimation of epicardial activation maps using sparse measurements from the intravenous catheters. The ultimate goal of this study was to determine the best number and location of pacing sites from which we should obtain the epicardial activation-time training maps (as a generalized training data set) so as to minimize the data acquisitions required. Our aim was to minimize the redundancy in the database and to be able to guide the eventual procedures required to obtain training data from open-chest surgery patients.

The general goal of training data set selection is to determine the relevant data to employ in a prediction algorithm (in our case statistical estimation) in the situation in which there is more data than necessary. The assumption is that in most cases all data are not equally useful in the training phase of a learning algorithm. Starting from a data set consisting of all the data, training set selection algorithm finds a suitable subset to be used in the learning algorithm. In the context of machine learning,

this concept is referred to as data reduction. The main problem of data reduction or scaling down data, in machine learning is how to select the relevant data for a particular problem. Data reduction can be achieved in two main ways: by selecting features or by selecting patterns. In this study, our focus will be the selection of patterns (a subset of the full data set) in data reduction.

Subset generation (or selection) is a search procedure that produces candidate subsets for evaluation based on a certain search strategy. Different search strategies have been developed until now: complete, sequential, and random search. The ones we were interested in were the sequential and random search algorithms. The sequential search can be classified in three categories: sequential forward selection, sequential backward elimination, and bidirectional selection. These approaches add or remove features or patterns one at a time. Another alternative includes the addition (or removal) of certain number of patterns in one step. Algorithms with sequential search are fast and simple to implement. On the other hand, random search algorithms include the generation of the next subset in a completely random manner. This approach uses randomness to escape local optima in the search space. The detailed descriptions of these methods can be found in Refs. [14,22]. Especially, the methods on ordered removal and addition and random search inspired the approaches we developed in this research.

In this study, our specific hypothesis was that there was a redundancy in the full training data set and the number of maps necessary for successful estimation could be reduced. For this purpose, we examined the best number of activation maps to be included in a general purpose training set. Specifically, we present five approaches, which examined sequential addition and removal of maps to select a generalized training set for the estimation technique. The selection consisted of choosing a subset of epicardial ectopic activation-time maps from a large database of beats which resulted in estimation accuracy levels better than or at least similar to using all the maps in database. We tested our approaches using a separate test set, thus determined the number of beats to be included as a generalized training set. The results of these tests showed that including only one third of the activation maps in our database would result in similar or even in some cases better estimation accuracy when compared to using all the maps in the database and, moreover, suggest that such an approach is feasible for providing accurate reconstruction of complete epicardial activation-time maps in a clinical setting.

2. Methods

In this study, we performed 14 dog experiments with various interventions, which were approved by our institution’s animal care and use committee, to create an epicardial activation-time map database. This database included a total of 592 epicardial activation maps. In all the experiments, we used a 490-electrode sock array (average inter-electrode distance was 4.3 mm) to record epicardial electrograms from dog hearts. We fabricated the sock from a piece of nylon stocking material mounted on a plaster mold of a dog heart. The locations of the coronary

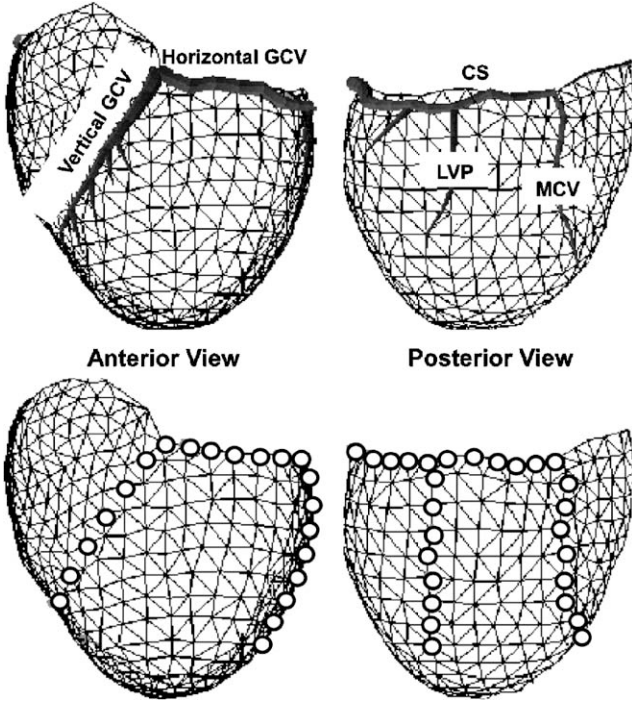


Fig. 1. A diagram representing the 490-electrode epicardial sock. The 490 electrodes are located in the nodes of the mesh; the 42 leads used as a surrogate catheter subset are indicated by larger dots. The top row contains the anterior and posterior view of the sock including coronary vessels and the lower row shows the sets of nodes on the sock corresponding to the 42-lead subset. The vessels we used include great cardiac vein (GCV), the coronary sinus (CS), the left ventricular posterior vein (LVP), and the middle cardiac vein (MCV).

vessels, from which we defined the 42-lead surrogate venous catheter subset, were also indicated on the mold, as shown in Fig. 1. The maps in our database were separated into two sets; training and test data sets. The training data set was obtained by electrically stimulating (pacing) a total of 470 different ventricular sites (maps with 239 right ventricular (RV) and 231 left ventricular (LV) pacing sites) in 12 dogs. Selecting a single map from each pacing site removed any bias that might come from over-representation of any activation pattern in the estimation process. The purpose of using single site stimulation in both of the training and test sets was to simulate the early activation that occurs from exit sites in reentry and focal activation that occurs in ectopic tachycardias. Ninety percent of the maps came from healthy hearts. However, in some experiments we also applied interventions that included localized heating and cooling, infusion of ethanol into a coronary artery, and a five-day-old infarction. The test set included data from two experiments (53 maps with RV and 69 with LV pacing sites): (1) 75 healthy, single pacing site maps from two different experiments, (2) 47 single pacing site maps with an ethanol injected heart.

The custom-built measurement system for the study was capable of sampling and saving continuously to magnetic disk up to 1024 channels with 1 kHz sampling rate and 12-bit resolution. Processing of the resulting recordings consisted of

selecting one representative and relatively high-quality beat from each 3-s recording. Determination of activation times was by means of finding the time of the minimum slope during the QRS complex of each of the electrograms. When the signal quality was low due to poor contact or broken leads, we applied wave-equation-based interpolation [23] to compute the potential values at the locations where measured data were not available. We then manually checked each resulting activation map for anomalous features or obvious errors using our custom-built visualization software *map3d* [24].

2.1. Linear estimation algorithm

Details of the estimation algorithm have been reported elsewhere [25]. Briefly, we first defined a training database consisting of up to 470 activation-time maps and selected the surrogate catheter leadset (42 leads) as a subset of the 490-lead sock. We assumed that those 42 leads contained “known” values (surrogates for the venous catheter leads) and the remaining 448 leads (for which we wished to estimate values) contained “unknown” activation values. We reordered the training set in such a way that the activation times for a given beat were treated as elements of a column vector, and then the various beats stacked side-by-side to form a matrix, \mathbf{AT} , such that the known values comprised the first 42 rows of the matrix. We then calculated the covariance matrix, \mathbf{K} , by the equation,

$$\mathbf{K} = \frac{(\mathbf{AT} - \overline{\mathbf{AT}})(\mathbf{AT} - \overline{\mathbf{AT}})^T}{\mathbf{N}}, \quad (1)$$

where \mathbf{N} is the number of maps in the training set.

The covariance matrix is central to the estimation approach we used. Hence, it is important to appreciate its contents and meaning. The covariance of two datasets (data from measurement site \mathbf{i} and \mathbf{j}) can be defined as their tendency to vary together. The covariance value will be larger than 0 if data from \mathbf{i} and \mathbf{j} tend to increase together, below 0 if data from \mathbf{i} tends to decrease as the data from \mathbf{j} increase, and 0 if they are uncorrelated (independent if Gaussianity applies). The covariance matrix consists of the variances of the variables along the main diagonal and the covariances between each pair of variables in the other matrix positions. The covariance matrix contains the covariance between each of the columns of a data matrix. That is, row \mathbf{i} and column \mathbf{j} of the covariance matrix represent the covariance between row (or column) \mathbf{i} and row (or column) \mathbf{j} of the original matrix. The diagonal elements are the variances of the rows (or columns) and the covariance matrix is symmetric.

We then formed an estimation matrix, \mathbf{E} , to be used to estimate the activation-times at the unmeasured sites as,

$$\mathbf{E} = \mathbf{K}_{\mathbf{uk}}^T \mathbf{K}_{\mathbf{kk}}^{-1}, \quad (2)$$

where $\mathbf{K}_{\mathbf{kk}}$ and $\mathbf{K}_{\mathbf{uk}}$ are submatrices of \mathbf{K} representing the auto-covariance of the known leads and the cross-covariance of known and unknown leads, respectively. \mathbf{E} is a matrix of basis vectors unique to the training set such that left multiplication by \mathbf{E} of any measurement vector of the 42 leads (with some manipulation to take care of the means, see Eq. (2), yields an

estimate of the activation values at all remaining sites and thus a complete, high-resolution map.

$$\mathbf{AT}_U^i = \mathbf{E} \times (\mathbf{AT}_K^i - \overline{\mathbf{AT}_K}) + \overline{\mathbf{AT}_U}, \quad (3)$$

where \mathbf{AT}_U^i and \mathbf{AT}_K^i are the measured and estimated portions, respectively, i th map. $\overline{\mathbf{AT}_K}$ and $\overline{\mathbf{AT}_U}$ are the rows of the first column of \mathbf{AT} that correspond to the known and unknown leads, respectively. In the computation of the inverse of \mathbf{K}_{kk} , we used the truncated singular-value decomposition technique [26] when the condition number (ratio between the largest and smallest singular value) of the \mathbf{K}_{kk} matrix was greater than 100,000. The number of singular values used in the truncation was set equal to the number of largest singular values whose summation comprised 99.1% of the cumulative sum of all of them.

2.2. Testing paradigms and error metrics

To evaluate the performance of the estimator, we used a “separate-test-set” protocol (STest), in which training data did not include any maps from the hearts that were used to obtain test data. This protocol represents the anticipated clinical application of the estimation method most closely. Comparing the test map to the associated estimate for each of the maps in the database provided a means of computing overall statistics that included beats from a range of pacing sites. The Euclidean distance between the actual and the estimated site of earliest activation, LDist, served as an index for error in each map estimation. The LDist is thereby a specific and clinically relevant measure based on the anticipated use of such a procedure.

2.3. Generalized training data set selection

To find a generalized training data set, we investigated five different selection methods, which were adopted from the data reduction literature in machine learning. The first method, which we referred to as “single-map-addition,” consisted of adding one map at a time to an initial training set with 10 maps whose pacing sites were evenly distributed over the epicardium. The addition metric was the mean LDist and the selection algorithm had four steps: (1) add one map from the full database (one out of remaining 460 maps in the first iteration); (2) apply estimation using the maps included in the current training set (11 maps in the first iteration) on the separate test set (122 maps used in STest testing paradigm); (3) compute mean LDist over the test maps; and (4) repeat steps 1–3 and determine the map whose addition resulted in the best performance (minimum mean LDist). We performed the addition until the training set contained all the maps in the full database.

The second training set selection method, which we referred to as “random-ten-maps-addition,” used a similar addition approach with a slight modification. In this method we added maps in groups of 10 which were selected randomly from the full database. The steps in this algorithm included (1) generation of 30 sets of 10 unique maps for each addition, (2)

selection of the maps whose addition gave the best performance in terms of earliest activation site determination (mean LDist), and (3) repetition of the first steps for the remaining maps in the full database. The goal of adding batches of maps was to increase the speed of selection. We experimented with different number of sets and number of maps in each set and found 30 sets and 10 maps in each set to perform the best.

The third method, which we referred to as “single-map-removal,” consisted of removing one map at a time from the 470-map training set and training the estimation matrix with the remaining maps (469 in the first iteration). We then determined the map whose removal yielded the minimum mean LDist and removed it from the data set from which additional selection occurred. The next iteration applied the same concept with the remaining maps and determined the map that would be removed. The removal process continued until the number of maps in the training data set was 10.

The fourth method, which we referred to as “random-ten-maps-removal,” removed 10 random maps from the database at each iteration instead of removing one map at a time. In the removal of 10 random maps we tried 30 different sets and determined the 10-map set whose removal resulted in the best mean LDist value and removed it; the remaining 460 maps were used in the second iteration, in which we selected 30 new random sets and determined the set to be removed, and so on. The test set was always the same for evaluating the training data set.

The fifth method, on the other hand, which we referred to as “spatial covariance-based removal,” was based on the training data set itself and the spatial covariance of the measurement sites using the training set. In this approach, we first obtained the spatial covariance using all the maps in the training database and then removed each map from this set one-by-one and computed the spatial covariance of the one-map-removed set. We compared the rows of the all-maps covariance matrix and each covariance matrix from the one-map-removed set (490-by-490 matrices) using correlation coefficient. We could determine the least contributing map to the spatial covariance by finding the largest average correlated set and thus the removed map. In the next iteration we removed one map from the remaining 469 maps, computed the spatial covariance matrix and performed the correlation comparison to determine the least contributing map. This algorithm stopped when the number of maps was 10.

Examining the plots of mean LDist vs. number of maps gave us the number of maps to be included in the generalized training set, which would yield an estimation accuracy level close to or better than that was obtained using all the maps in the full database. We also present estimation results and spatial covariance maps to compare different training set contents obtained with different approaches.

3. Results

The correlation between those maps in the training database (470 maps) that had nearby pacing sites was quite high. We computed the correlation coefficients (“CC”) by comparing

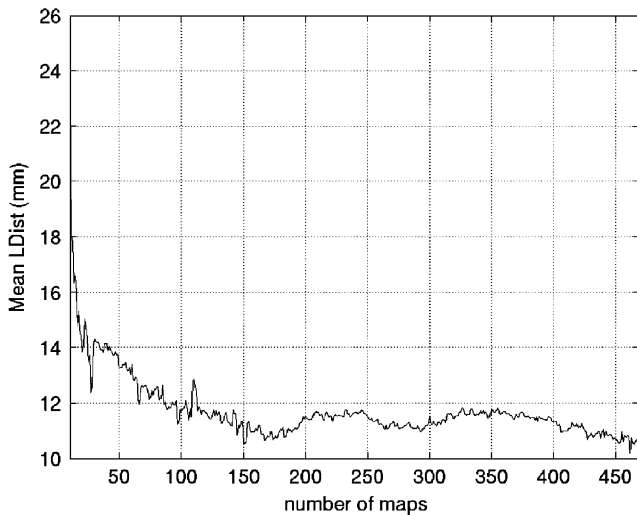


Fig. 2. Generalized training data set selection using the single-map-addition method. Axes are the mean LDist vs. the number of maps used in the training.

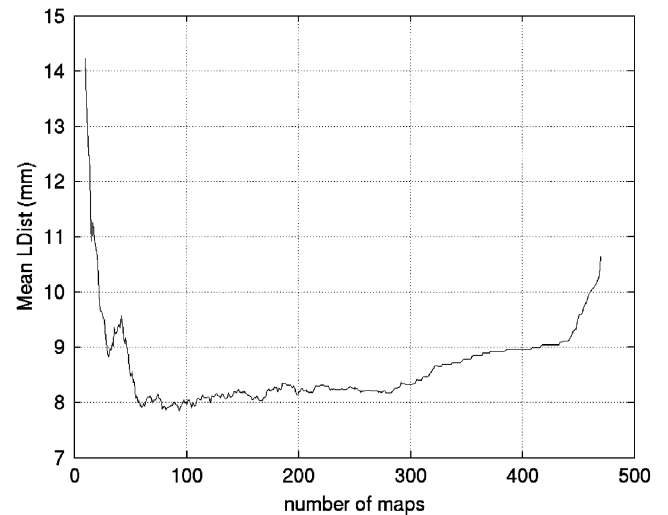


Fig. 4. Generalized training data set selection using the single-map-removal method for four different trials.

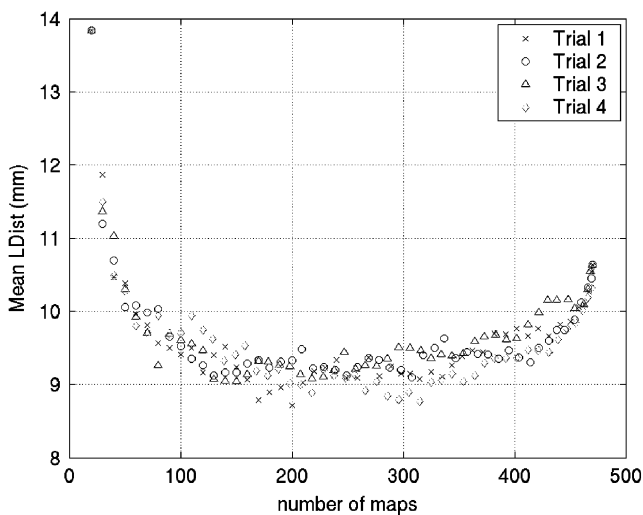


Fig. 3. Generalized training data set selection using the random-ten-maps-addition method for four different trials.

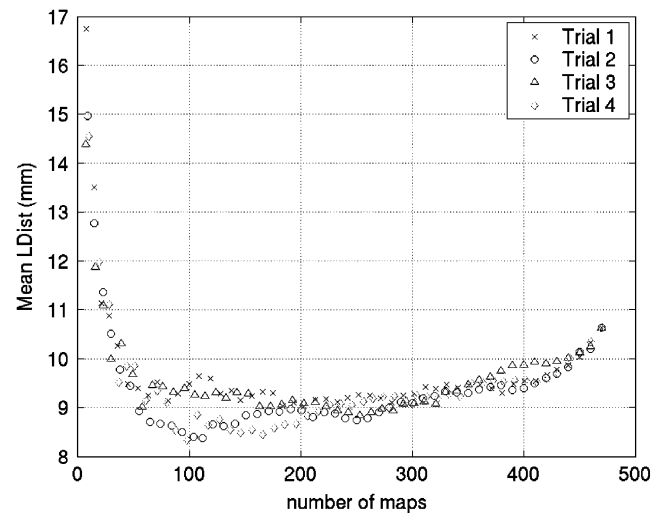


Fig. 5. Generalized training data set selection using the random-ten-maps-removal method for four different trials.

each map with the maps whose pacing sites were the closest to pacing site of that map and determined the mean of CC for each map. The maximum of mean CCs was 0.99, minimum was 0.64, and mean was 0.91. In addition, we found that 97% of the maps had a CC that was greater than 0.80. When we compared the maps from different experiments but paced from the same site (totally 83 comparisons), mean CC was 0.88 (max 0.98 min 0.65) which showed the high correlation of ectopic foci maps even when they came from different hearts. These results indicated the redundancy in this database and motivated the need for determining the set of maps in the training data that minimized redundancy yet still maintained the best performance.

Fig. 2 shows the mean LDist values with respect to the number of added maps using the single-map-addition method. With only 150 maps we could obtain an LDist value (10.8 mm) similar to that when using all the maps in the database. After the

further addition of approximately 100 maps, the mean LDist did not change significantly and oscillated between 10.5 and 12 mm. This general selection method was based on including all possible combinations of maps in the training set one-by-one and evaluating them on the separate test set, therefore, it was time-consuming (approximately 70 h of computation on SGI workstations with two 300 MHz processors).

Fig. 3 shows the relationship between mean LDist values and the number of maps added using the random-ten-maps-addition method. The figure includes the results from four different trials of random batch (10 maps at a time) selections, which were not very different from each other. They showed a parabolic-shape relationship, i.e., for small and very large number of maps mean LDist values were high while medium-size training sets (from 130 to 370 maps) performed better and determined the earliest activation sites in a vicinity of approximately 9 mm.

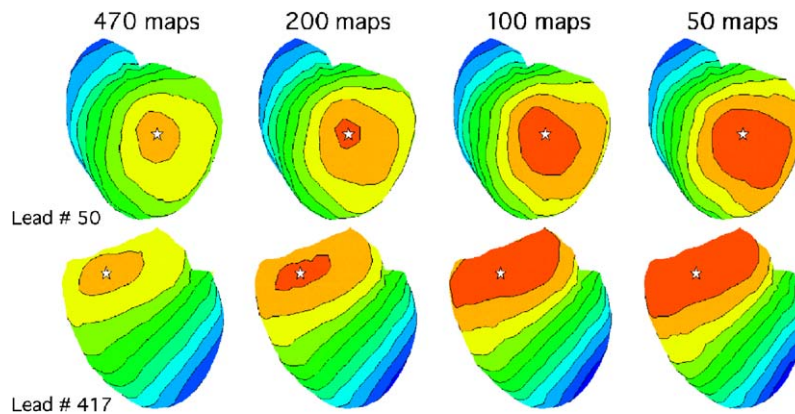


Fig. 6. Sets of spatial covariance patterns from two leads (shown with stars; one on the left ventricle and one on the right ventricle) for different number of maps selected using the spatial covariance-based removal method. The numbers of maps selected were 470, 200, 100, and 50 from left to right, respectively. The same scaling was used for each pattern. The covariance values are high on the regions that are close to the star, becomes zero at distant sites, and go to negative values on the opposite side of the heart.

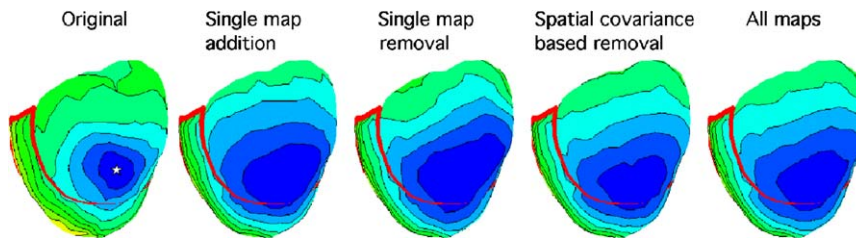


Fig. 7. Examples of estimation results using 100 maps selected with the single-map-removal, single-map-addition, and spatial covariance-based removal methods and all the maps in the training database. Blue shows the early activated region and each contour corresponds to 10 ms increments in the activation times.

In terms of computational power, the batch selection methods were more efficient and less time consuming (approximately 45 min of computation on the same processors).

As shown in Fig. 4, in the single-map-removal method removal of maps improved estimation until the number of maps was around 100 and estimation error stayed in a similar range until there were 70 maps in the training set, after which the mean LDist increased with the removal of additional maps. This method resulted in a mean LDist of 7.9 mm with 100 maps compared to 10.6 mm with 470 maps (2.7 mm improvement on average). This was also a highly time consuming method (approximately 70 h of computation). Fig. 5 shows a similar pattern of first improvement and then degradation in performance as we removed the maps from the full training database using the random-ten-maps-removal method. Again, at around 100 maps the mean LDist values were lowest. A further decrease in the number of maps in the training set below 70, resulted in mean LDist increasing, indicating a critical threshold in the number of maps included in the training set. The computation took approximately 45 min on the same processors.

In the spatial covariance-based removal method, performance did not change significantly until the number of maps was around 150. A slight decrease in the mean LDist values occurred as we decreased the number of maps to 70. When the maps were fewer than 70, the estimation resulted in 12.5 mm and worse mean LDist. The computation took approximately 50 h on the same processors.

Fig. 6 contains sets of spatial covariance patterns from two leads (shown with stars; one on the left ventricle and one on the right ventricle) for different number of maps selected using the spatial covariance-based removal method. The numbers of maps selected were 470, 200, 100, and 50 from left to right, respectively. The resulting spatial covariance patterns were not significantly different from each other. The selection algorithm was based on the correlation coefficient and the mean correlation coefficient between the full database covariance matrices and covariance matrices computed with 50 maps was approximately 0.99. The covariance values are high on the regions that are close to the star (pacing site), becomes zero at relatively distant sites, and go to negative values on the opposite side of the heart.

Fig. 7 contains a set of original and estimated maps using either 100 maps selected with the single-map-removal, single-map-addition, and spatial covariance-based removal methods or all the maps in the training database (470 maps). This figure shows the similar performance of the four training sets, one of size 100 and the other 470 on a test map with a pacing site on the posterior right ventricle. Black (blue in color version) represents the early activated region and each contour corresponds to approximately 10 ms increments in the activation times.

4. Discussions

The aim of this study was to develop strategies for determining the optimal number of maps in generalized training data

sets for estimation of epicardial activation-time maps from intravenous catheter measurements. The driving hypothesis was that there was a redundancy in the full training data set and the number of maps necessary for successful estimation could be reduced. For this purpose, we examined the problem of optimal number of epicardial activation maps to be included in a general purpose training set so as to minimize the data acquisitions required. Our aim was to minimize the redundancy in the database and to be able to guide the eventual procedures required to obtain training data from open-chest surgery patients. The results from this study illustrated the redundancy in our database and suggested that by including an optimal subset of the full database the estimation technique was able to perform as well as and even in some cases better than including all the maps in the database.

Specifically, we proposed five different approaches for determining the optimal number of maps with minimal redundancy and the best performance to be included in the generalized training set and consistently found that around 100 maps with unique pacing sites on the epicardium could be used in the training set to estimate the high-resolution activation-time maps for epicardially originating ectopic activity. Using a subset of the full database of activation maps brought about a 2.7 mm improvement in determining the earliest activation site. Even though the performances of different approaches were quite similar, the single-map-removal approach performed the best among all five methods.

Our study has focused entirely on beats paced from the epicardium, even though the bulk of clinical catheter mapping concentrates on the endocardium. The motivation for this choice was that for an important percentage of patients with post-myocardial infarction and nonischemic sustained ventricular tachycardias, uniquely endocardial approaches do not provide successful determination of target sites and may even lead to reoccurrence of arrhythmias after endocardial ablation procedures [3,5,27]. In addition, there now exist the required devices and technical experience to routinely probe the coronary veins in patients with up to 20 electrodes on a single catheter. Clinicians already make use of the information from these catheters to reveal local electrical activity in arrhythmia cases but are unable to identify and localize events that occur more than a few millimeters from the veins. Perhaps most compelling, once there is adequate evidence to suggest epicardial involvement, there are also methods by which to bring radio-frequency ablation catheters to the critical sites and carry out treatment. Therefore, there exists both a need to develop techniques for mapping epicardial arrhythmias and an emerging diagnostic technology that could lead to a treatment paradigm. We note also that the techniques we have developed would almost certainly work equally well when applied to the endocardial surface as an activation mapping tool, perhaps enabling more rapid mapping of unstable dynamic rhythms from fewer catheter measurements. We concentrated in this study on epicardial mapping even though the approaches we describe also apply to endocardial mapping.

Limitations of this study include that the database did not include data from hearts with large regions of conduction block

or in which we observed re-entry. Preliminary (unpublished) results from a small number of test beats with large areas of previous myocardial infarction suggest that while localizing the earliest site of activation may be feasible, there will be difficulties in predicting the entire activation sequence when the infarcted regions lie far from the venous catheters. Ongoing experiments will provide the data to develop training sets that include such profoundly altered hearts.

Although we have shown that this approach to epicardial mapping is quite feasible and accurate, its application to clinical practice will require overcoming additional technical hurdles. Perhaps the first is the need to acquire high-resolution epicardial maps with which to build the necessary database. Obtaining such data does require direct access to the heart. However, open-chest surgery is still a relatively frequent occurrence for such procedures as valve repair and replacement and coronary artery bypass grafts. The time required during such procedures to obtain epicardial maps is just minutes, so that it might not present substantial additional burden to the patient. Another alternative for the creation of the training database might be to use simulated activation-time maps from a numerical/computational model with different pacing sites under different conditions. Specifically, we would use a heart model; by which it is possible to simulate large number of activation-time maps to obtain endocardial, midmyocardial, and epicardial values to feed into the statistical estimation machine.

An additional challenge to applying this technique in a clinical setting will be determining the relationship between venous catheter locations and the corresponding sites in the high-density epicardial sock array. For this, we anticipate using fluoroscopic images obtained during the catheterization procedure. A study into the impact of estimation error in localizing electrode locations is currently underway in our laboratory.

Moreover, we did not deal directly with different sized hearts, even though we used different animals with various heart sizes. However, using a flexible nylon sock compensated this phenomenon in terms of training data gathering. Warping and morphing techniques, which have to include changing the propagation as well as size, might be the alternative approaches to address this problem faced by the estimation approach.

The results of this study encourage further investigation and provide adequate evidence that an epicardial mapping approach based on intravenous catheter measurements is feasible and can provide adequate accuracy for clinical applications. With the advances in transthoracic access to the pericardial space in order to apply catheter ablation of cardiac arrhythmias [28,29], such an estimation approach will complement this type of treatment as a minimally invasive diagnostic technique.

5. Summary

Minimally invasive catheter-based cardiac mapping techniques that are limited to the endocardium are unsuccessful when the origin of the arrhythmia is located deep in the subendocardium or in the subepicardium, which is the case in 15% of all ventricular arrhythmias. However, electrophysiological studies targeting the epicardium are limited to regions

near the coronary vessels or require transthoracic access. We have developed a statistical approach by which to estimate high-resolution maps of epicardial activation from very low-resolution multielectrode venous catheter measurements. This technique uses a linear estimation model that derives a relationship between venous catheter measurements and unmeasured epicardial sites from a set of previously recorded, high-resolution epicardial activation-time maps used as a training data set based on the spatial covariance of the measurement sites. The general purpose training data set selection consisted of choosing a subset of epicardial activation-time maps from a database that could be used in all possible test cases with focal ectopic activity. The ultimate goal of this particular study was to determine the best number and location of pacing sites from which we should obtain the epicardial activation-time training maps (as a generalized training data set) so as to minimize the data acquisitions required. Our aim was to minimize the redundancy in the database and to be able to guide the eventual procedures required to obtain training data from open-chest surgery patients. The training set selection consisted of choosing a subset of epicardial activation-time maps which resulted in estimation accuracy levels better than or at least similar to using all the maps in database.

In this study, we performed 14 dog experiments with various interventions to create an epicardial activation-time map database. This database included a total of 592 epicardial activation maps. In all the experiments we used a 490-electrode sock array (average inter-electrode distance was 4.3 mm) to record epicardial electrograms from dog hearts. The training data set was obtained by electrically stimulating (pacing) a total of 470 different ventricular sites in 12 dogs. The test set included 122 maps from two experiments which were different from the ones included in the training data set.

In this study, our hypothesis was that there was a redundancy in the full training data set and the number of maps necessary for successful estimation could be reduced. To find a generalized training data set, we investigated five different selection methods, which were adopted from the data reduction literature in machine learning. The first method, which we referred to as single-map-addition, consisted of adding one map at a time to an initial training set. In the second method (random-ten-maps-addition), we added maps in groups of 10 which were selected randomly from the full database. The third method (single-map-removal) consisted of removing one map at a time from the 470-map training set and training the estimation matrix with the remaining maps. The fourth method (random-ten-maps-removal) removed 10 random maps from the database at each iteration instead of removing one map at a time. The fifth method (spatial covariance-based removal) was based on the training data set itself and the spatial covariance of the measurement sites using the training set. We could determine the least contributing map to the spatial covariance by finding the largest average correlated set and thus the removed map.

Our results showed that 100 maps would be sufficient to obtain an estimation accuracy level that was better than all the maps paced from all over the epicardium which brought about a

2.7 mm improvement in determining the earliest activation site. Even though the performances of different approaches were quite similar, the single-map-removal approach performed the best among all five methods.

The results of this study encourage further investigation and provide adequate evidence that an epicardial mapping approach based on intravenous catheter measurements is feasible and can provide adequate accuracy for clinical applications. With the advances in transthoracic access to the pericardial space in order to apply catheter ablation of cardiac arrhythmias, such an estimation approach will complement this type of treatment as a minimally invasive diagnostic technique.

Acknowledgments

We gratefully acknowledge Dr. Bruno Taccardi, Dr. Bonnie B. Punske, Dr. Phil Ershler, Jayne Davis, Matt Allison, and Bruce Steadman at the CVRTI, for their assistance in the animal experiments. We thank Dr. Dana H. Brooks at Northeastern University, Boston, MA, for his helpful suggestions. We extend thanks to Dr. Jeroen Stinstra at the CVRTI for his thoughtful contributions in our discussions. The support for this work comes from the Whitaker Foundation, the Nora Eccles Treadwell Foundation, and the Richard A. and Nora Eccles Harrison Fund for Cardiovascular Research.

References

- [1] American Heart Association, Heart diseases and stroke statistics-2003 update, Technical Report, American Heart Association, Dallas, Texas, 2002.
- [2] W. Kaltenbrunner, R. Cardinal, M. Dubuc, M. Shenasa, R. Nadeau, G. Tremblay, M. Vermeulen, P. Savard, P.L. Page, Epicardial and endocardial mapping of ventricular tachyarrhythmia in patients with myocardial infarction, Is the origin of the tachycardia always subendocardially localized?, *Circulation* 84 (1991) 1058–1071.
- [3] E. Sosa, M. Scanavacca, A. d'Avila, F. Pilleggi, A new technique to perform epicardial mapping in the electrophysiology laboratory, *J. Cardiovasc. Electrophysiol.* 7 (1996) 531–536.
- [4] J. Brugada, A. Berruezo, A. Cuesta, J. Osca, Nonsurgical transthoracic epicardial radiofrequency ablation, An alternative in incessant ventricular tachycardia, *J. Am. Coll. Cardiol.* 41 (2003) 2036–2043.
- [5] R.A. Schweikert, W.I. Saliba, G. Tomassoni, N.F. Marrouche, C.R. Cole, T.J. Dressing, P.J. Chou, D. Bash, S. Beheiry, C. Lam, L. Kanagaratnam, A. Natale, Percutaneous pericardial instrumentation for endo-epicardial mapping of previously failed ablations, *Circulation* 108 (2003) 1329–1335.
- [6] A. d'Avilla, P. Gutierrez, M. Scanavacca, V. Reddy, D.L. Lustgarten, E. Sosa, J.A.F. Ramires, Effects of radiofrequency pulses delivered in the vicinity of the coronary arteries: Implications for nonsurgical transthoracic epicardial catheter ablation to treat ventricular tachycardia, *PACE* 25 (2002) 1488–1495.
- [7] M.D. Arruda, K. Otomo, C. Tondo, J. Pitha, H. Nakagawa, J. Bussey, R. Lazzara, W. Jackman, Epicardial left ventricular mapping and RF catheter ablation from the coronary veins: a potential approach for ventricular tachycardia, *PACE* 18 (1995) 857.
- [8] A.A. de Paola, W.D. Melo, M.Z. Tavora, E.E. Martinez, Angiographic and electrophysiological substrates for ventricular tachycardia mapping through the coronary veins, *Heart (CEN)* 79 (1998) 59–63.
- [9] R.O. Kuenzler, R.S. MacLeod, B. Taccardi, Q. Ni, R.L. Lux, Estimation of epicardial activation maps from intravascular recordings, *J. Electrocardiol.* 32 (1999) 77–92.

- [10] B. Yılmaz, R.S. MacLeod, S. Shome, B.B. Punske, B. Taccardi, Minimally invasive epicardial activation mapping from multielectrode catheter, in: Proceedings of the IEEE Engineering in Medicine and Biology Society 23rd Annual International Conference, 2001, pp. 290–293.
- [11] I. Guyon, J. Makhoul, R. Schwartz, V. Vapnik, What size test set gives good error rate estimates?, *IEEE Trans. Pattern Anal. Mach. Intell.* 20 (1998) 52–64.
- [12] H.M. Kalayeh, D.A. Landgrebe, Predicting the required number of training samples, *IEEE Trans. Pattern Anal. Mach. Intell.* 5 (1983) 664–666.
- [13] J.S. Sanchez, R. Barandela, A.I. Marques, R. Alejo, J. Badenas, Analysis of new techniques to obtain quality training sets, *Pattern Recogn. Lett.* 24 (2003) 1015–1022.
- [14] J.R. Cano, F. Herrera, M. Lozano, Using evolutionary algorithms as instance selection for data reduction in KDD: Experimental study, *IEEE Trans. Evol. Comput.* 7 (2003) 561–575.
- [15] P.N. Belhumeur, J.P. Hespanha, D.J. Kriegman, Eigenfaces vs. fisherfaces: Recognition using class specific linear projection, *IEEE Trans. Pattern Anal. Mach. Intell.* 19 (1997) 711–720.
- [16] S.V. Beiden, M.A. Maloof, R.F. Wagner, A general model for finite-sample effects in training and testing of competing classifiers, *IEEE Trans. Pattern Anal. Mach. Intell.* 25 (2003) 1561–1569.
- [17] J.C. Bezdek, L.O. Hall, L.P. Clarke, Review of MR image segmentation techniques using pattern recognition, *Med. Phys.* 20 (1993) 1033–1048.
- [18] D. Scholz, N. Fuhs, M. Hixson, An evaluation of several different classification schemes, their parameters, and performance, in: Proceedings of the 13th International Symposium on Remote Sensing of the Environment, Ann Arbor, University of Michigan, 1979, pp. 399–405.
- [19] M. Hixson, D. Scholz, N. Fuhs, Evaluation of several schemes for classification of remotely sensed data, *Photogramm. Eng. Remote Sensing* 46 (1980) 1547–1553.
- [20] S. Tadjudin, D.A. Landgrebe, Covariance estimation with limited training samples, *IEEE Trans. Geosci. Remote Sensing* 37 (1999) 2113–2118.
- [21] B. Yılmaz, R.S. MacLeod, B.B. Punske, B. Taccardi, D.H. Brooks, Venous catheter based mapping of epicardial ectopic activation: Training set selection for statistical estimation, *IEEE Trans. Biomed. Eng.* 52 (2005) 1823–1831.
- [22] H. Liu, L. Yu, Toward integrating feature selection algorithms for classification and clustering, *IEEE Trans. Knowl. Data Eng.* 17 (2005) 1–12.
- [23] Q. Ni, R.S. MacLeod, R.L. Lux, B. Taccardi, A novel interpolation method for electric potential fields in the heart during excitation, *Ann. Biomed. Eng.* 26 (1998) 597–607.
- [24] R.S. MacLeod, C.R. Johnson, Map3d: interactive scientific visualization for bioengineering data, in: Proceedings of the IEEE Engineering in Medicine and Biology Society 15th Annual International Conference, IEEE Press, New York, 1993, pp. 30–31.
- [25] Y. Serinağaoğlu, R.S. MacLeod, B. Yılmaz, D.H. Brooks, Multielectrode venous catheter mapping as high quality constraint for electrocardiographic inverse solutions, *J. Electrocardiol.* 35 (Suppl.) (2002) 65–73.
- [26] W.H. Press, B.P. Flannery, S.A. Teukolsky, W.T. Vetterling, *Numerical Recipes: The Art of Scientific Computing*, Cambridge University Press, Cambridge, New York, Melbourne, 1986.
- [27] V. Swarup, J.B. Morton, M. Arruda, D.J. Wilber, Ablation of epicardial macroreentrant ventricular tachycardia associated with idiopathic nonischemic dilated cardiomyopathy by a percutaneous transthoracic approach, *J. Cardiovasc. Electrophysiol.* 12 (2002) 1164–1168.
- [28] C. Vahlhaus, H.J. Bruns, J. Stypmann, T.D. Tjan, F. Janssen, M. Schafers, H.H. Scheld, O. Schober, G. Breithardt, T. Wichter, Direct epicardial mapping predicts the recovery of left ventricular dysfunction in chronic ischaemic myocardium, *Eur. Heart J.* 25 (2004) 151–157.
- [29] F. Ouyang, D. Bansch, A. Schaumann, S. Ernst, C. Linder, P. Falk, H. Hachiya, K.H. Kuck, M. Antz, Catheter ablation of subepicardial ventricular tachycardia using electroanatomic mapping, *Herz* 28 (2003) 591–597.

Bülent Yılmaz received the BS ('97) and MS ('99) degrees in Electrical and Electronics Engineering from Middle East Technical University, Ankara, Turkey, and the Ph.D. degree (2004) from University of Utah, Salt Lake City, Utah. He is currently an Assistant Professor and Vice Chairman of Biomedical Engineering at Başkent university, Ankara, Turkey. His research interests are in biomedical signal and image processing.

Robert S. MacLeod received both the BS ('79) degree in engineering physics and the PhD ('90) degree in physiology and biophysics from Dalhousie University, Halifax, NS Canada. He received the MS degree in electrical engineering from the Technische Universität, Graz, Austria, in 1985. He is an Associate Professor in the Bioengineering Department and the Department of Internal Medicine (Division of Cardiology) at the University of Utah, Salt Lake City, and an associate director of the Scientific Computing and Imaging Institute and the Nora Eccles Harrison Cardiovascular Research and Training Institute. His research interests include computational electrocardiography (forward and inverse problems), experimental investigation and clinical detection of cardiac ischemia and repolarization abnormalities, and scientific computing and visualization.